https://doi.org/10.5194/hess-2019-560
Preprint. Discussion started: 18 November 2019

Hydrology and Earth System Sciences
Discussions

Multi-constellation GNSS interferometric reflectometry with mass-market sensors as a solution for soil moisture monitoring

Angel Martín[1], Sara Ibáñez[2], Carlos Baixauli[3], Sara Blanc[4], Ana B. Anquela[1]

[1]Department of Cartographic Engineering, Geodesy and Photogrammetry, Universitat Politècnica de Valencia, Valencia, 46022, Spain
[2]Centro Valenciano de Estudios sobre el Riego, Universitat Politècnica de Valencia, Valencia, 46022, Spain
[3]Cento de Experiencias Cajamar, Paiporta, Valencia, 46200, Spain
[4]Institute of Information and Communication Technologies boratory Universitat Politècnica de Valencia, Valencia, 46022, Spain.

Correspondence to: Angel Martín (aemartin@upvnet.upv.es)

Abstract. Per capita arable land is decreasing due to rapidly increasing population, and fresh water is becoming scarce and more expensive. Therefore, farmers should continue to use technology and innovative solutions to improve efficiency, save input costs, and optimise environmental resources (such as water). In the case study presented in this manuscript, the GNSS-IR technique was used to monitor soil moisture during 66 days, from December 3, 2018, to February 6, 2019, in the installations of the Cajamar Centre of Experiences, Paiporta, Valencia, Spain. Two main objectives were pursued. The first was the extension of the technique to a multi-constellation solution using GPS, GLONASS, and GALILEO satellites, and the second was to test whether mass-market sensors could be used for this technique. Both objectives were achieved. At the same time the GNSS observations were made, soil samples taken at 5 cm depth were used for soil moisture determination to establish a reference dataset. Based on a comparison with that reference data set, all GNSS solutions, including the three constellations and the two sensors (geodetic and mass-market), were highly correlated, with a correlation coefficients between 70% and 85%.

1 Introduction

Soil moisture is a fundamental component of the hydrological cycle, and a key observable variable for optimising agricultural irrigation management. Additionally, soil moisture monitoring has been one of the main goals of the remote sensing satellite missions Soil Moisture and Ocean Salinity (SMOS), (Kerr et al., 2001), Soil Moisture Active Passive (SMAP), (Chan et al. 2016), and Sentinel-1, (Mattia et al., 2018). SMOS is used to derive global maps of soil moisture every three days at a spatial resolution of about 50 km, SMAP every two-three days with a spatial resolution of about 10 km, and Sentinel-1 every two-three days with a spatial resolution of about 1 km.

To obtain information about soil moisture at a very local scale and continuously, Global Navigation Satellite System (GNSS) reflectometry began to be tested as a possible solution (Masters et al., 2002; Zavorotny et al., 2003; Katzberg et al., 2005). This was possible because GNSS satellites transmit in the L-band (microwave frequency), so the GNSS signal reflected by

https://doi.org/10.5194/hess-2019-560
Preprint. Discussion started: 18 November 2019


Hydrology and Earth System Sciences
Discussions

nearby surfaces and recorded by the antenna contains information about the environment surrounding the antenna (scale of about 1000 m2). In particular, the ground-reflected global positioning system signal measured by a geodetic-quality GNSS system can be used to infer temporal changes in near-surface soil moisture. This technique, known as GNSS-interferometric reflectometry (GNSS-IR), analyses changes in the interference pattern of the direct and reflected signals, (Fig. 1), which are recorded in signal-to-noise ratio (SNR) data, as interferograms. Temporal fluctuations in the phase of the interferogram are indicative of changes in near-surface (depth of about 5-7 cm) volumetric soil moisture content, (Larson et al., 2008a, 2008b). Commercially available geodetic-quality GNSS receivers and antennas can be used for GNSS-IR. The method has been tested with the Global Positioning System (GPS) satellite constellation, and it has been shown to provide consistent measurements of upper surface soil moisture content, (Larson et al., 2008a, 2008b, 2010; Larson and Nievinski, 2013; Chew et al., 2014, 2015, 2016; Small et al., 2015, Vey et al., 2015; Wan et al., 2015; Chen et al., 2016; Zhang et al., 2017).

The GNSS-IR footprint for a single rising or setting satellite is an elongated ellipse in the direction of the satellite track (Fresnel ellipse or zones; Larson et al., 2010; Wan et al., 2015; Vey et al., 2015; Roesler and Larson, 2018). As the satellite rises and the elevation angle increases, the Fresnel zone becomes smaller and closer to the GNSS antenna. Data with elevation angles higher than 30 degrees should be discarded from the SNR series because they contain no significant oscillations and cannot be retrieved reliably. Data with elevation angles lower than 5 degrees should also be discarded in order to avoid strong multipath effects from trees, artificial surfaces, and structures surrounding the antenna. A GNSS satellite takes about one hour to rise from an elevation angle of 5 degrees to an angle of 30 degrees.

With the use of the GPS constellation, the GPS-IR reflection footprint is far from homogeneous, as shown in Fig. 2, and some tracks cannot be included in the process and analysis (Vey et al., 2015; Chew et al., 2016). Therefore, GPS-IR needs to evolve to Global Navigation Satellite System reflectometry, GNSS-IR, where multi-constellation observation provides the solution. The integration of new navigation satellite constellations will produce a more homogeneous footprint around the antenna (Fig. 2). Roussel et al. (2016) introduced the GLONASS Russian constellation to retrieve soil moisture over bare soil, but there are no references in the literature for the European GALILEO or Chinese BEIDU constellations. Roesler and Larson (2018) provided a software tool for generating map GNSS-IR reflection zones that support GPS, GLONASS, GALILEO, and BEIDU constellations.

Therefore, the first objective of this research was to extend the GPS-IR methodology to a multi-constellation scenario (GPS, GLONASS, and GALILEO; BEIDU is not introduced in this research), which will produce a much larger sample set of observations around the antenna, as shown in Fig. 2, than is obtained with only the GPS constellation.

Additionally, geodetic-quality GNSS receivers and antennas are an expensive solution. If we keep in mind that the final market will be the agricultural market, a technique developed using those devices will never be introduced into the sector. Thus, the second objective of this research was the introduction of mass-market GNSS sensors as the basis for the technique. If the use of these mass-market devices can be confirmed, it will be possible to use several of them at the same time to add redundancies in the processing at a very low cost.

https://doi.org/10.5194/hess-2019-560
Preprint. Discussion started: 18 November 2019

Hydrology and Earth System Sciences
Discussions

2 Materials and methods

2.1 Location of the experiment

The experiment was conducted in the installations of the Cajamar Centre of Experiences, located in Paiporta, Valencia, Spain (39°25´3´´ N, 0°25´4´´ W), which is an agricultural research technology centre (https://www.fundacioncajamarvalencia.es/es/comun/actividades/ in Spanish).

The centre began its activities in 1994. Some of the research topics carried out by the centre are the valorisation of agricultural by-products and the use of microorganisms in food, pharmaceuticals, and aesthetics using the latest biotechnology resources; the design of new containers and bio-functional formats for the marketing of healthy foods with high added value; improvement in irrigation automation, biological control management, and agronomic management in organic production; and the introduction of alternative value crops and new varieties that guarantee the sustainability of our sector.

2.2 Instrumental and observations

A geodetic GNSS receiver (Trimble R10 GNSS receiver, from the Department of Cartographic Engineering Geodesy and Photogrammetry of the Universitat Politècnica de València) and a mass-market receiver (Navilock GNSS receiver based on a u-blox 8 UBX-M8030-KT chipset with a built-in antenna) connected to a Raspberry Pi 3 for use as a control device and for storing the observations, were used to obtain multi-constellation SNR observables (GPS, GLONASS and GALILEO). Five seconds sample rate observations were obtained simultaneously for both sensors (Fig. 3).

The frequencies used in the experiments were L1, for the GPS and GLONASS satellite constellations and E1 for the GALILEO constellation. This choice was forced because the mass-market device could not track the L2 or E5 satellite signals. However, Vey et al. (2011) showed that the soil moisture root mean square difference between L2C and L1 was only 0.03 m^3/m^3.

The geodetic GNSS receiver saves the observations (including SNR data) in the commonly used RINEX files, so the elevation and azimuth of a satellite for an epoch should be computed from the observation RINEX file and the navigation RINEX file, (Hofmann-Wellenhof et al., 2008).

The mass-market receiver uses NMEA GSV sentences to provide integer numbers for elevation, azimuth and signal-to-noise ratio (SNR) directly.

The results were compared with soil moisture measurements based on soil samples taken at a depth of 5 cm and weighed before and after being dried (gravimetric method) in a laboratory (Fig. 4). These measurements were considered the reference dataset.

In total, 66 days of measurements, from December 3, 2018, to February 6, 2019, were observed, processed, and analysed. The height of the antennas from the ground was 1.80 m for the geodetic GNSS device and 1.84 m for the mass-market device.

https://doi.org/10.5194/hess-2019-560
Preprint. Discussion started: 18 November 2019


Hydrology and Earth System Sciences
Discussions

Precipitation data were added in the final plot results. These data were obtained from a meteorological station located in the Cajamar Experiences Centre (100 meters from the GNSS antennas).

2.3 Theoretical background

The theoretical background is based on the procedure developed by Larson et al., (2010) and detailed in Chew et al., (2014), vey et al., (2015), and Zhang et al., (2017). Only full-tracks data covering more than 30 minutes and cover more than 10 degrees of elevation in its trajectory were considered in our study. Each valid track of a satellite was separated into ascending path and descending path.

The processing of each satellite track can be summarised as follows:

1) SNR data are converted from dB units to linear scale in volts using the conversion equation (S stands for SNR in the next equation and for the rest of equations in the manuscript) $S_{lineal}=10^{S/20}$ (vey et el., 2016).
2) A low-order polynomial (second degree) is fit to the S_{lineal} in order to eliminate the direct satellite signal, so that the reflected signal is isolated: $S_{lineal}^{reflected}$, (Wan et al., 2015; Chew et al., 2016).
3) A Lomb-Scargle periodogram (Lomb, 1976; Press et al., 1992; Roesler and Larson, 2018), is then computed from $S_{lineal}^{reflected}$, and the track goes to the next step only if there is a clear signal that reflects a primary wave. Tracks with multiple peaks or low maximum average power (less than four times the background noise) are not included in the next step. If the Lomb-Scargle periodogram is computed using the sine elevation angle as the input X axis, the result converts the frequency into antenna height in the output X axis. Only tracks with computed antenna height consistent with the measured antenna height (less than 0.1 meters difference), go to the next step.
4) The selected tracks are modelled using the expression below:

$$S_{lineal}^{reflected} = A\cos\left(\frac{4\pi h}{\lambda}\sin e + \emptyset\right) \qquad (1)$$

The equation means that $S_{lineal}^{reflected}$ can be modelled in terms of the amplitude A and phase offset ϕ of a primary wave. λ is the GNSS wavelength (L1 for GPS and GLONASS and E1 for GALILEO), e is the satellite elevation, and h is the antenna height, which is assumed to be a constant due to the low signal penetration on the ground (Chew et al., 2014; Roussel et al., 2016; Zhang et al., 2017). The least squares algorithm (Strang and Borre, 1997; Leick et al., 2015) is used to estimate A and ϕ.

5) Chew et al., (2013) derived a linear relationship between the previously computed phase offset and soil moisture with a slope of 65.1°. We used this value to convert the phase values of each track into GNSS-derived volumetric water content, VWG_{GNSS} (m^3/m^3), V stands for VWG in the next equation and for the rest of equations in the manuscript:

https://doi.org/10.5194/hess-2019-560
Preprint. Discussion started: 18 November 2019


Hydrology and Earth System Sciences
Discussions

$$V_{GNSS} = \frac{\Delta\emptyset_t}{65.1} + V_{Residual} \qquad (2)$$

where $V_{Residual}$ is the minimum soil moisture observation from the reference data set (from the soil samples). This minimum value should be taken from the reference observations as long as the GNSS observation is continuous and uncut. In the case that there is any cut in the GNSS observation data, this value must be chosen again among the reference values after the cut. $\Delta\emptyset_t = \emptyset - \emptyset_o$ is calculated with respect to a reference phase $\emptyset_o$ computed in this work as proposed by Chew et al. (2016): the mean of the lowest 15% of the computed phases for each satellite tracks during the retrieval period. $\emptyset_o$ should be computed again in the case of cut of the GNSS signal. Ascending and descending paths for the same satellite are treated separately.

However, Zhang et al. (2017) showed that it is important to adjust the linear relationship with the test data in order to obtain better results (their results showed a decrease of the final standard deviation from 0.036 m^3m^{-3} -using the linear relationship of 65.1°- to 0.008 m^3m^{-3}).

6) Finally, the mean of all satellite tracks of the same constellation that pass at different times during the day is computed, so the final GNSS soil moisture represents a temporal average for all observations analysed during one day. To address the objectives of this research, we have three different results, one for each GNSS constellation.

3 Results

3.1 Pre-processing

RINEX observation and navigation files from the geodetic GNSS antenna were used to generate the input file for the processing process. This file contained year, month, day, hour, satellite identification, SNR, elevation, and azimuth for every observed epoch. We computed three different files (GPS, GALILEO and GLONASS). In contrast to GPS or GALILEO, GLONASS satellites transmit carrier signals at different frequencies. The L1 frequencies are:

$$f_{L1} = f_O + k * \Delta f_{L1} \qquad k = 1,2,\ldots.24, \qquad (3)$$

where f_o = *1602.0 MHz,* and $\Delta f_{L1} = 0.5625\ MHz$, and k is the carrier number assigned to the specific GLONASS satellite (Hoffmann et al., 2008). Thus, the frequency for each satellite should be computed and included in the GLONASS file.

The file containing the NMEA observations from the mass-market antenna was used to generate three different input files for the processing process, one for each satellite constellation. However, due to the integer nature of the SNR, elevation, and azimuth observation numbers, an extra pre-processing step was included for the mass-market observation files. This step

https://doi.org/10.5194/hess-2019-560
Preprint. Discussion started: 18 November 2019


Hydrology and Earth System Sciences
Discussions

used the navigation files from the International GNSS Service (IGS) repository (http:/www.igs.org) to obtain float numbers for elevation and azimuth values.

160

3.2 Processing

The processing followed the steps defined in the previous section.

The geodetic antenna SNR data in volts for satellite GPS 23 are shown in Fig. 5a, the SNR data with the direct signal removed are shown in Fig. 5b, the Lomb-Scargle periodogram for the SNR reflected signal is shown in Fig. 5c, and the SNR
165 reflected signal with the adjusted wave (Step 4 in the previous section) is shown in Fig. 5d. Fig. 6 portrays the same concepts for the same satellite but using the mass-market antenna observations. Fig. 7 and 8 portray the same concepts for the GLONASS satellite 5, and Fig. 9 and 10 display these for the GALILEO satellite 21.

A linear relationship with a slope of 65.1° between the GNSS computed phase offset and the soil moisture was used, but two different values for $V_{Residual}$ and $\emptyset_o$ were used due to an outage of the electrical power during three days (from day 40 to day
170 42 of the experiment). No observations were recorded during those days.

Fig. 11, 12, and 13 show a comparison of the daily soil moisture from GPS, GLONASS, and GALILEO, respectively, where the results of the geodetic and mass-market antennas can be compared with the reference gravimetric data set. Daily precipitation amounts are also included in the figures.

4 Discussion

175 The numerical values for Fig. 11, 12, and 13 are listed in Table 1, where the RMS and the correlation between the GNSS antennas and the reference values are shown. The best results were obtained for the GLONASS constellation, whose range of values appears more compressed for both the geodetic and mass-market antennas in comparison with the GPS and GALILEO results. The worst results were obtained for GALILEO constellation. However, the ranges between these results are less than 0.01 m^3/m^3 for RMS and 0.15 for correlation, so we can consider that the three constellations produce similar
180 V_{GNSS} values, as do the geodetic and mass-market antennas. Our RMS results using the a priori slope values of 65.1° are comparable with those obtained by Zhang et al. (2017), who processed six months of continuous observations and obtained a mean standard deviation value of 0.036 m^3/m^3, and those of Vey et al. (2015), who processed 6 years of observations and obtained a standard deviation value of 0.06 m^3/m^3.

The SNR values from the geodetic antenna and the mass-market antenna for the GPS constellation are similar, as suggested
185 in Li and Geng (2019), because the u-blox chipset uses an active, right-handed, circularly polarised antenna with uniform antenna gain. However, the SNR values for GLONASS and GALILEO present a systematic bias of about 3-5 db-Hz between the geodetic and mass-market antennas (Fig. 7a and 8a and Fig. 9a and 10a). This effect has an impact in the range of the

https://doi.org/10.5194/hess-2019-560
Preprint. Discussion started: 18 November 2019


Hydrology and Earth System Sciences
Discussions

reflected signal (Fig. 7b and 8b and Fig. 9b and 10b), but it has no effects in the final phase offset variations for the adjusted wave.

According to Step 3 of Section 2.3, the 70% of the GPS tracks recorded by the geodetic antenna were considered valid for processing, as were 73% for GALILEO, and 74% for GLONASS. This percentage is reduced to around a 10% if we consider the tracks recorded by the mass-market antenna. Nonetheless, one of the main important problems in this research is related with the selection of the correct tracks to be processed and adjusted using Step 4 of Section 2.3. Based on the mentioned criteria (tracks with multiple peaks or low maximum average power and computed reflector height consistent with the measured antenna height), some tracks that should not be processed are processed (around 8% of all tracks irrespective the constellation). These wrongly processed tracks introduce outliers in the computed V_{GNSS}, which are eliminated in the daily final mean V_{GNSS} computation because they produce a high RMS in the daily computations using all satellites. One way to accomplish this task could be to use good figures, such as those from Fig. 5c Fig. 5d, to produce a valid set of training images and use machine learning tools (image recognition) to decide automatically whether a new track can be considered as a good track (so it can be processed) or not. This idea is currently under development.

In situ observations are needed to solve Eq. 2 ($V_{Residual}$ parameter). However, if there are no reference values, this constant cannot be included, and the results will present an offset in comparison with the real values. However, the results can be used in a relative way, that is, can be used to infer VWC variations from one day to another. This relative comparison can be performed only if the observations are continuous. If there is an interruption in the raw data (because the antenna is turned off) of more than two or three hours, the previous reference is lost and the relative comparisons should start again (from the moment the antenna is turned on again). In situ observations are also needed if we want to adjust the linear relationship between the computed phase offset and the soil moisture, as is developed in Zhang et al. (2017); however, if there are no reference values, the slope value of 65.1° can also be used to obtain accurate results.

5 Conclusions

The case study presented in this research is focused on the GNSS SNR data acquisition and processing using the GNSS-IR technique to monitor soil moisture. The main objectives of this research were the use and comparison of GPS, GLONASS, and GALILEO constellations solutions and the use and comparison of a geodetic and mass-market antenna solutions.

Independent GPS, GLONASS, and GALILEO solutions were generated to demonstrate that the technique can be extended to a multi-constellation solution. This is necessary because a single constellation solution presents a reflection footprint that is far from homogeneous around the antenna and because 30-35% of the observed satellite tracks of the geodetic antenna are not valid for processing (40-45% if the mass-market antenna is considered).

The use of a mass-market GNSS antenna was confirmed to be a viable tool for GNSS-IR, with the caution of using the IGS navigation files to transform the observed integer numbers obtained in the NMEA messages for the elevation and azimuth of the satellites into floating numbers. With the use of mass-market sensors, it will become possible to design scenarios with

https://doi.org/10.5194/hess-2019-560
Preprint. Discussion started: 18 November 2019


Hydrology and Earth System Sciences
Discussions

several GNSS stations generating redundant observations. Therefore, maps of soil moisture variations by specific and selective areas of soil, cultivation, and/or management can be generated, instead of obtaining only an average value for the entire observation area.

GNSS-IR is still a technique with numerous technological challenges in order to becoming a competitive solution with respect to current observation techniques, but it has great potential with regard to continuity of observation (can be implemented in a real or quasi-real time scenario), precision, and measurement acquisition cost if mass-market antennas are used.

Data availability

GNSS raw observations used to conduct this study are available upon request from the corresponding author (Angel Martin)

References

Chan, S. K., Bindlish, R., O'Neill, P. E., Njoku, E., Jackson, T., Colliander, A., Chen, F., Burgin, M., Dunbar, S., Piepmeier, J., Yueh, S., Entekhabi, D., Cosh, M. H., Caldwell, T., Walker, J., Wu, X., Berg, A., Rowlandson, T., Pacheco, A., McNairn, H., Thibeault, M., Martínez-Fernández, J., González- Zamora, A., Seyfried, M., Bosch, D., Starks, P., Goodrich, D., Prueger, J., Palecki, M., Small, E. E., Zreda, M., Calvet, J.- C., Crow, W., and Kerr, Y.: Assessment of the SMAP passive soil moisture product, IEEE T. Geosci. Rem. Sens., 54, 4994–5007, 2016.

Chen, Q., Won, D., Akos, D.M., and Small, E.E.: Vegetation using GPS interferometric reflectometry: experimental results with a horizontal polarized antenna, IEEE J. Select. Top. Appl. Earth Obs. Rem. Sens., 9(10), 4771-4780, 2016.

Chew, C.C., Small, E.E., Larson, and K.M., Zavorotny, V.U.: Effects of near-surface soil moisture on GPS SNR data: development and retrieval algorithm for soil moisture, IEEE T. Geosci. Rem. Sens., 52(1), 537-543, 2014.

Chew, C.C., Small, E.E., Larson, K.M., and Zavorotny, U.Z.: Vegetation sensing using GPS-interferometric reflectometry: theoretical effects of canopy parameters on signal-to-noise ratio data, IEEE T. Geosci. Rem. Sens., 53(5), 2755-2764, 2015.

Chew, C.C., Small, E.E., and Larson, K.M.: An algorithm for soil moisture estimation using GPS-interferometric reflectometry for bare and vegetated soil, GPS Solut., 20(3), 525-537, 2016.

Hofmann-Wellehof, B., Lichtenegger, H., and Wasle, E.: GNSS Global Navigation Satellite Systems, GPS, GLONASS, GALILEO and more, Ed. SpringerWienNewYork 2008.

Katzberg, S.J., Torres, O., Grant, M.S., and Masters, D.: Utilizing calibrated GPS reflected signals to estimate soil reflectivity and dielectric constant: results from SMEX02, Rem. Sens. Environ., 100(1), 17-28, 2005.

Kerr, Y., Waldteufel, P., Wigneron, J., Martinuzzi, J., Font, J., and Berger, M.: Soil moisture retrieval from space: The Soil Moisture and Ocean Salinity (SMOS) mission, IEEE T. Geosc. Rem. Sens., 39, 1729-1735, 2001.

https://doi.org/10.5194/hess-2019-560
Preprint. Discussion started: 18 November 2019

250 Larson, K.M., Small, E.E., Gutmann, E. D., Bilich, A.L., Axelrad, A., and Braun, J.J.: Using GPS multipath to measure soil moisture fluctuations: initial results, GPS solut., 12(3), 173-177, 2008a.

Larson, K.M., Small, E.E., Gutmann, E. D., Bilich, A.L., Braun, J.J., and Zavorotny, V.U.: Use of GPS receivers as a soil moisture network for water cycle studies, Geophys. Res. Lett., 35, L24405, 2008b.

Larson, K.M., Braun, J.J., Small, E.E., and Zavorotny, V.U.: GPS multipath and its relation to near-surface soil moisture 255 content, IEEE J. Selec. Top. Appl. Earth Obs. Rem. Sens, 3(1), 91-99, 2010.

Larson, K.M., and Nievinski, F.G.: GPS snow sensing: results from the EarthScope plate boundary observatory, GPS solut., 17(1), 41-52, 2013.

Leick, A., Rapoport, L., and Tatarnikov, D.: GPS satellite surveying. John Wiley & Sons, fourth edition, 840 pp.

Li, G., Geng, J. (2019): Characteristics of raw multi-GNSS measurement error from Google Android smart devices, GPS 260 Solut., 23(3), https://doi.org/10.1007/s10291-019-0885-4, 2015.

Lomb, N.R.: Least-squares frequency-Analysis of unequally spaced data, Astrophys. Space Sci. 39(2), 447-462, 1976.

Masters, D., Axelrad, P., and Katzberg, S.: Initial results of land-reflected GPS bistatic radar measurements in SMEX02, Rem. Sen. Environ., 92(4), 507-520, 2002.

Mattia, F., Balenzano, A., Satalino, G., Lovergine, F., Peng, J., Wegmuller, U., Cartus, O., Davidson, M.W.J., Kim S., 265 Johnson, J., Walker, J., Wu, X., Pauwels, V.R.N., McNairn, H., Caldwell, T., Cosh, M., and Jackson, T: Sentinel-1 & Sentinel-2 for SOIL Moisture Retrieval at Field Scale, IGARSS 2018-2018 IEEE I. Geos. Rem. Sens. Symposium, https://doi.org/10.1109/IGARSS.2018.8518170.6147-6150, 2018.

Press, W.H., Teukolsky, S.S., Vetterling, W.T., and Flannery, B.P.: Numerical recipes in Fortran 77, vol. 1, 2nd edn. Cambirdge Uniersity Press, New York, pp 569-573, 1992.

270 Roesler, C., and Larson, K.M.: Software tools for GNSS interferometric reflectometry (GNSS-IR), GPS Solut., 22: 80. https://doi.org/10.1007/s10291-018-0744-8, 2018.

Roussel, N., Frappart, F., Ramillien, G., Darroes, J., Baup, F., Lestarquit, L., and Ha, M.C.: Detection of soil moisture variations using GPS and GLONASS SNR data for elevation angles ranging from 2º to 70º, IEEE J. Selec. Top. Appl. Earth Obs. Rem. Sens, 9(10), 4781-4794, 2016.

275 Small, E.E., Larson, K.M., Chew, C.C., Dong, J., and Ochsner, T.E.: Validation of GPS-IR soil moisture retrievals: comparison of different algorithms to remove vegetation effects, IEEE J. Selec. Top. Appl. Earth Obs. Rem. Sens, 9(10), 4759-4770, 2016.

Strang, G., and Borre, K.: Linear algebra, Geodesy and GPS. Wellesley-Cambride Press, 624 p, 1997.

Vey, S., Güntner, A., Wickert, J., Blume, T., and Ramatschi, M.: Long-term soil moisture dynamics derived from GNSS 280 interferometric reflectometry: a case study for Sutherland, South Africa. GPS Solut., DOI 10.1007/s10291-015- 0474-0, 2015.

Wan, W., Larson, K.M., Small, E.E., Chew, C.C., and Braun, J.J.: Using geodetic GPS receivers to measure vegetation water content, GPS solute., 19, 237-248, 2015.

https://doi.org/10.5194/hess-2019-560
Preprint. Discussion started: 18 November 2019

Zavorotny, V.U., Masters, D., Gasiewski, A., Bartram, B., Katzberg, S., Aselrad, P., and Zamora, R.: Seasonal polarimetric measurements of soil moisture using tower-based GPS bistatic radar, In: Proceedings of IEEE 2003 I. geos. Rem. Sens. symposium, IGARSS 2003, vol. 2, 781-783, 2003.

Zhang, S., Roussel, N., Boniface, K., Ha, M. C., Frappart, F., Darrozes, J., Baup, F., and Calvet, J.C.: Use of reflected GNSS SNR data to retrieve either soil moisture or vegetation height from a wheat crop, Hydrol. Earth Syst. Sci., 21, 4767-4784, 2017.

	GPS CONSTELLATION		GALILEO CONSTELLATION		GLONASS CONSTELLATION	
	Geodetic	Mass-market	Geodetic	Mass-market	Geodetic	Mass-market
RMS (m^3/m^3)	0.025	0.026	0.028	0.024	0.020	0.020
Correlation	0.77	0.72	0.75	0.76	0.83	0.84

Table 1. Comparison of the soil moisture estimates from GNSS with the reference values.

https://doi.org/10.5194/hess-2019-560
Preprint. Discussion started: 18 November 2019

Hydrology and Earth System Sciences
Discussions

320 **Figures**

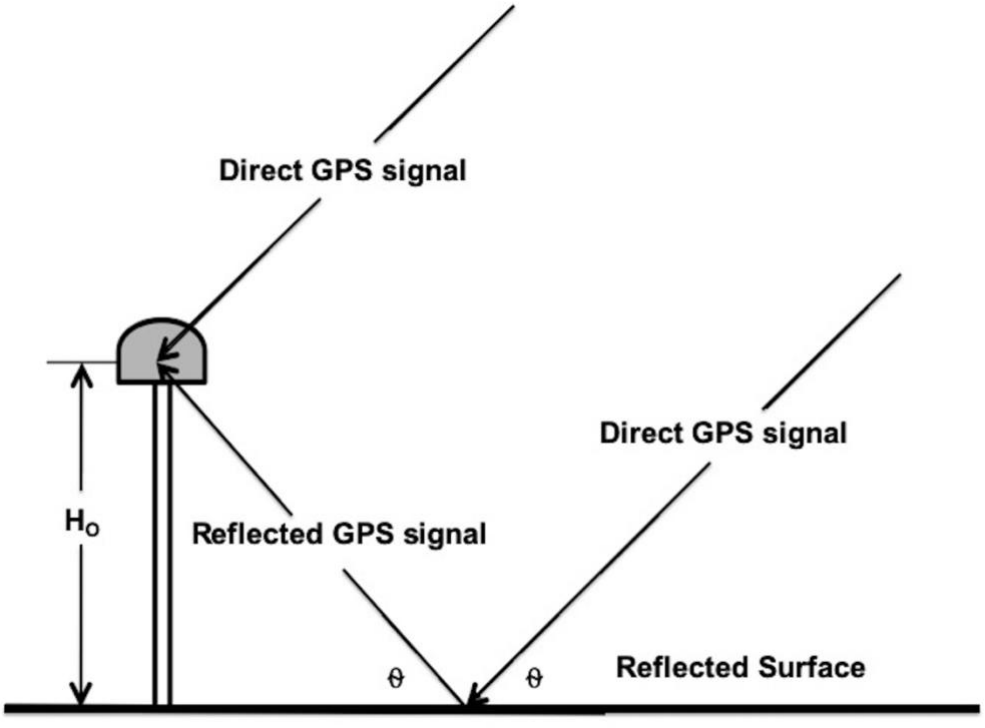

340 **Figure 1. Principle of Global Navigation Satellite System interferometric reflectometry (GNSS-IR). HO is the antenna height, and θ it the satellite elevation angle.**

https://doi.org/10.5194/hess-2019-560
Preprint. Discussion started: 18 November 2019

Hydrology and Earth System Sciences
Discussions

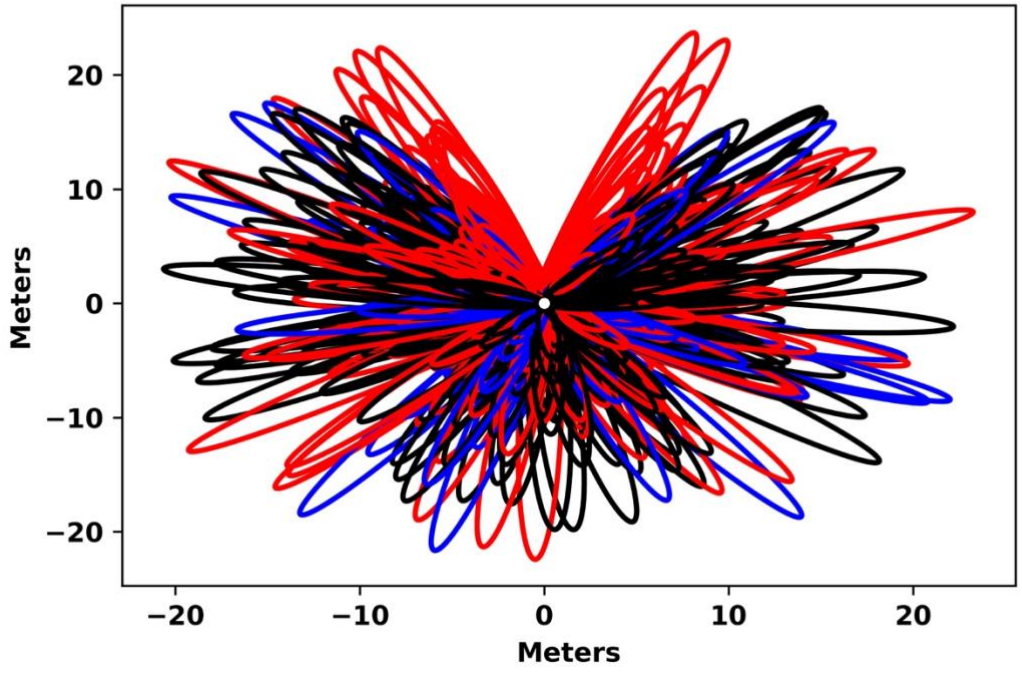

Figure 2. GNSS Fresnel ellipses around the geodetic antenna during one of the observation days. GPS constellations satellites are shown in black, GLONASS satellites are shown in red, and GALILEO satellites are shown in blue.

https://doi.org/10.5194/hess-2019-560
Preprint. Discussion started: 18 November 2019

Hydrology and Earth System Sciences
Discussions

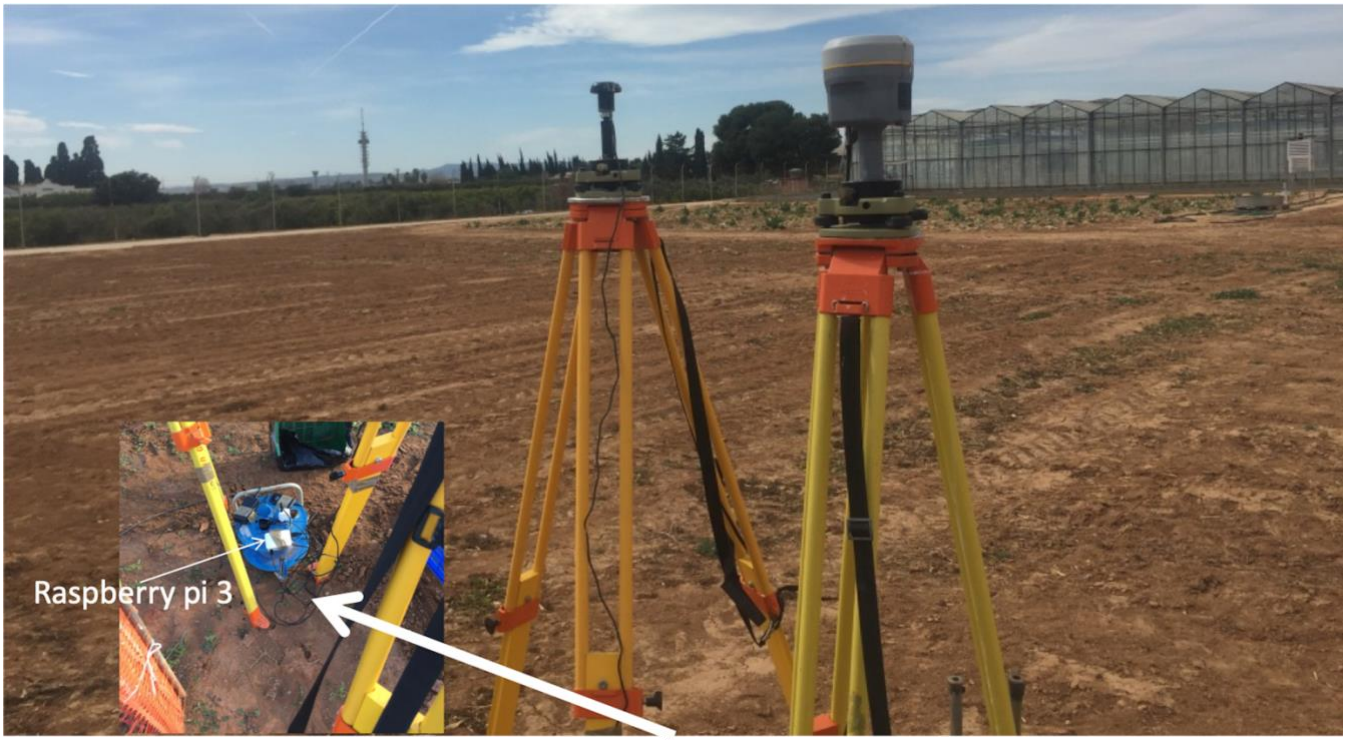

Figure 3. Instrumental configuration in the field campaign. A geodetic-quality GNSS antenna and a mass-market GNSS antenna were working at the same time.

https://doi.org/10.5194/hess-2019-560
Preprint. Discussion started: 18 November 2019

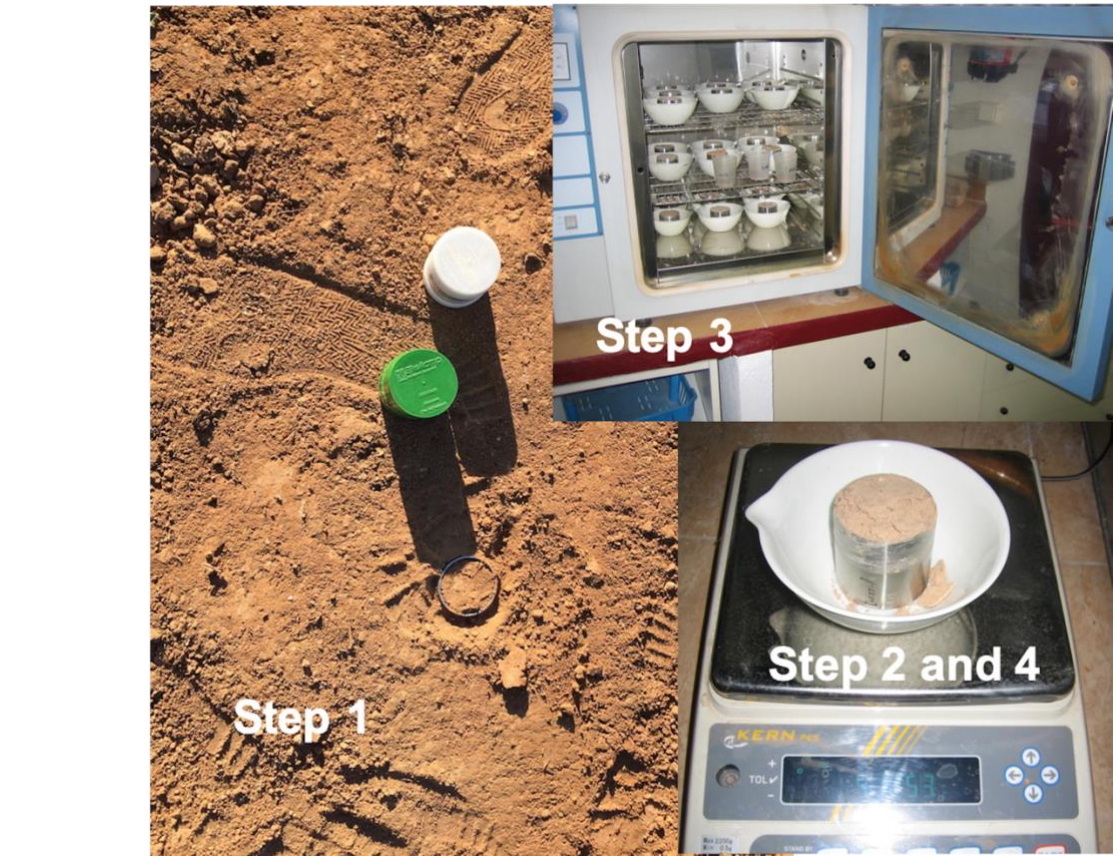

Figure 4. Gravimetry method used for producing a reference dataset. Step 1: taking the soil sample. Steps 2 and 4: weighing the sample. Step 3: drying the sample.

https://doi.org/10.5194/hess-2019-560
Preprint. Discussion started: 18 November 2019

Hydrology and Earth System Sciences
Discussions

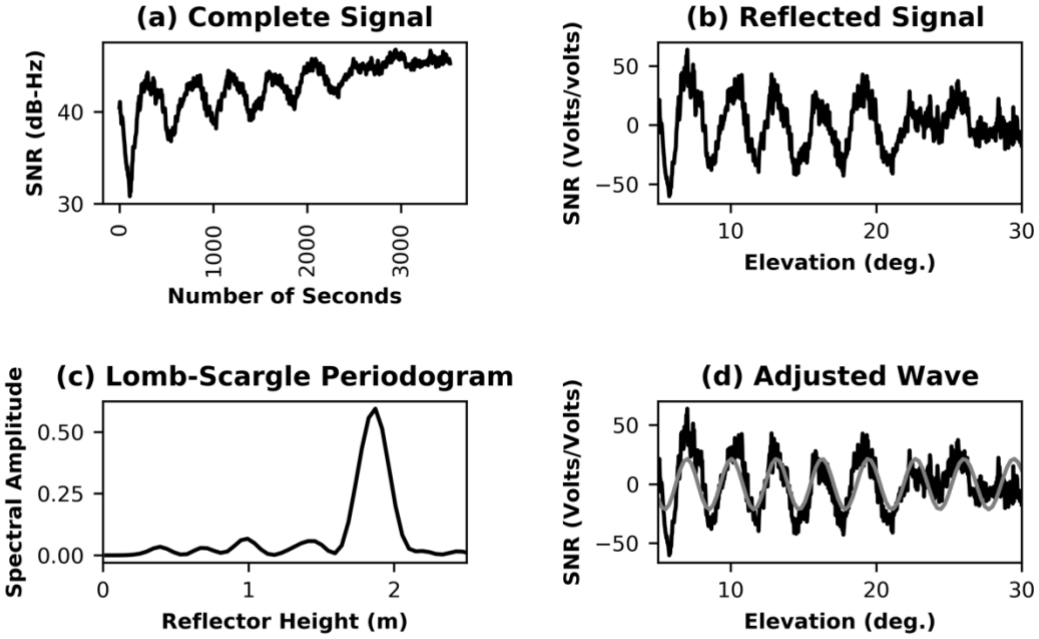

Figure 5. GPS satellite 23 observed with the geodetic antenna. a) SNR data in volts, b) SNR data with the direct signal removed, c) Lomb-Scargle periodogram for the SNR reflected signal, d) SNR reflected signal with the adjusted wave.

https://doi.org/10.5194/hess-2019-560
Preprint. Discussion started: 18 November 2019

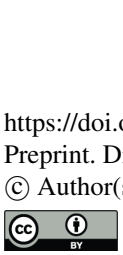

Hydrology and Earth System Sciences
Discussions

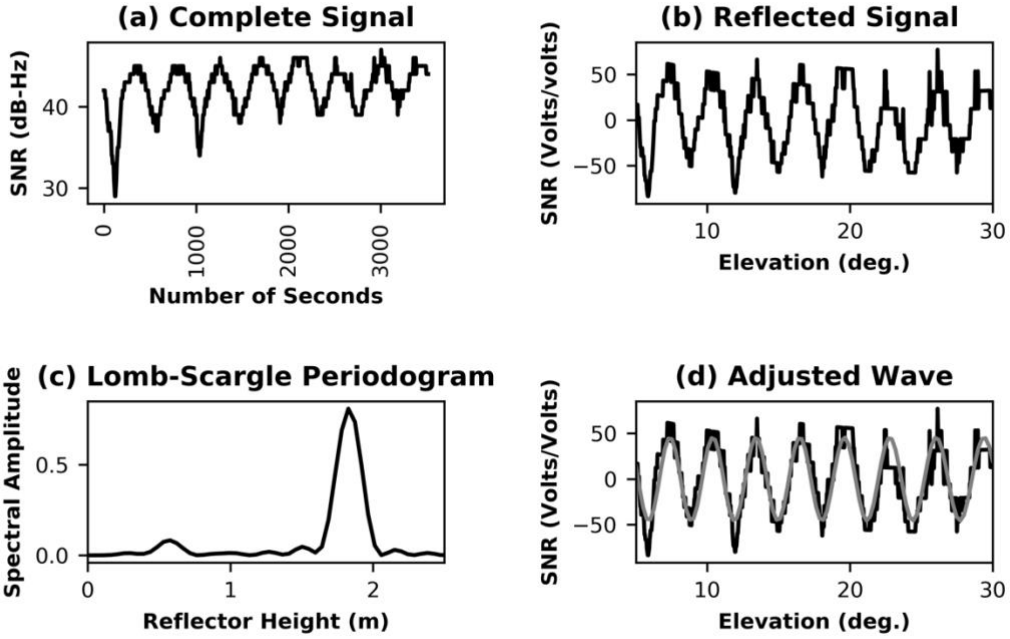

Figure 6. GPS satellite 23 observed with the mass-market antenna. a) SNR data in volts, b) SNR data with the direct signal removed, c) Lomb-Scargle periodogram for the SNR reflected signal, d) SNR reflected signal with the adjusted wave.

https://doi.org/10.5194/hess-2019-560
Preprint. Discussion started: 18 November 2019

Hydrology and Earth System Sciences
Discussions

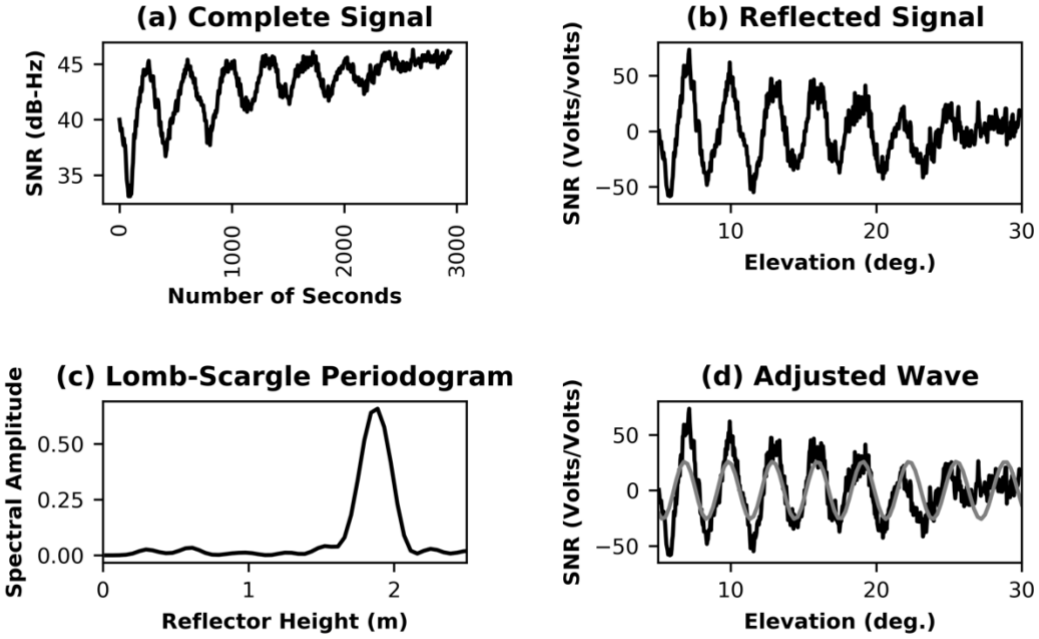

Figure 7. GLONASS satellite 5 observed with the geodetic antenna. a) SNR data in volts, b) SNR data with the direct signal removed, c) Lomb-Scargle periodogram for the SNR reflected signal, d) SNR reflected signal with the adjusted wave.

https://doi.org/10.5194/hess-2019-560
Preprint. Discussion started: 18 November 2019

Hydrology and Earth System Sciences
Discussions

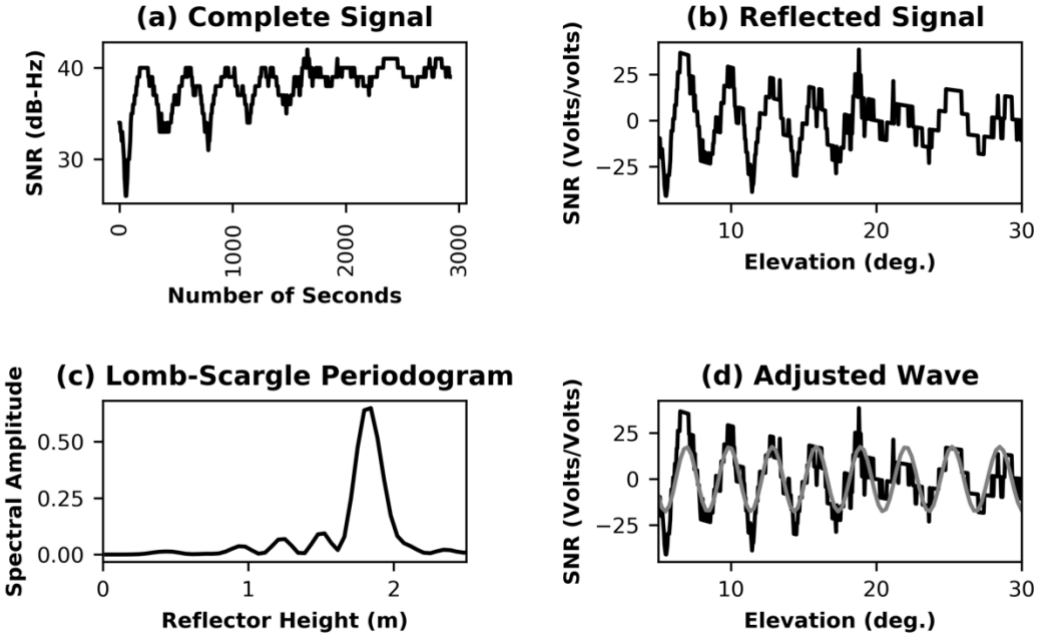

Figure 8. GLONASS satellite 5 observed with the mass-market antenna. a) SNR data in volts, b) SNR data with the direct signal removed, c) Lomb-Scargle periodogram for the SNR reflected signal, d) SNR reflected signal with the adjusted wave.

https://doi.org/10.5194/hess-2019-560
Preprint. Discussion started: 18 November 2019

Hydrology and Earth System Sciences
Discussions

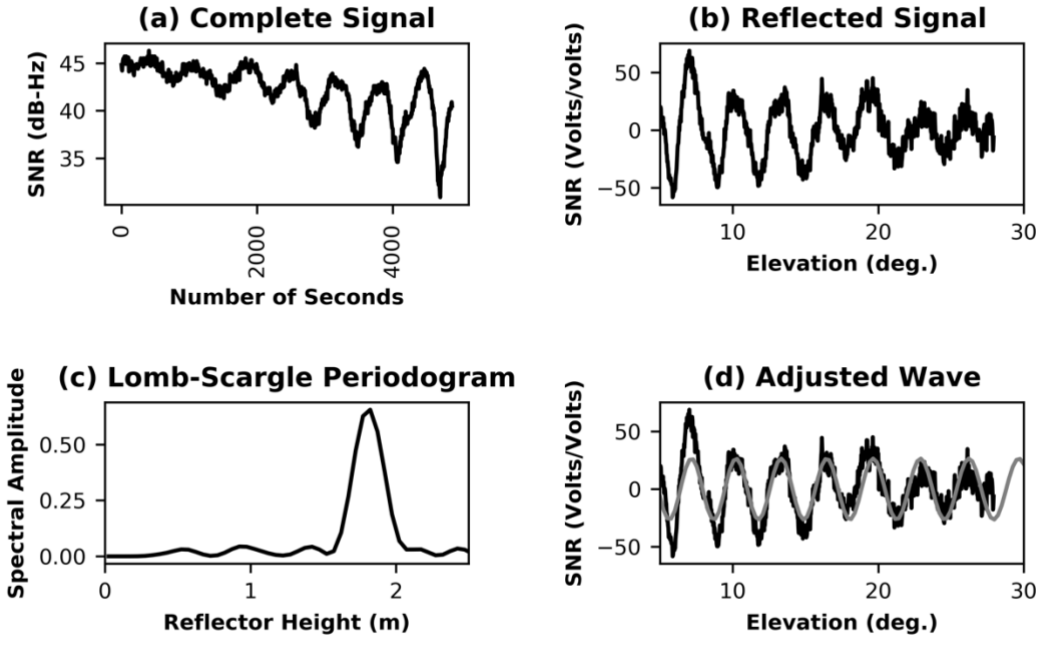

Figure 9. GALILEO satellite 21 observed with the geodetic antenna. a) SNR data in volts, b) SNR data with the direct signal removed, c) Lomb-Scargle periodogram for the SNR reflected signal, d) SNR reflected signal with the adjusted wave.

https://doi.org/10.5194/hess-2019-560
Preprint. Discussion started: 18 November 2019

Hydrology and Earth System Sciences
Discussions

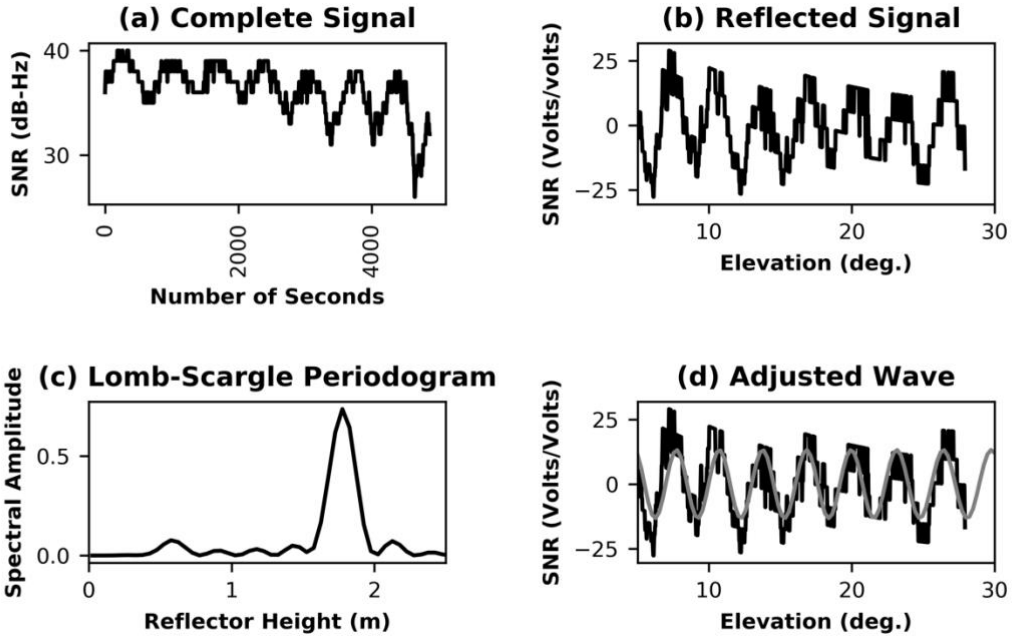

Figure 10. GALILEO satellite 21 observed with the mass-market antenna. a) SNR data in volts, b) SNR data with the direct signal removed, c) Lomb-Scargle periodogram for the SNR reflected signal, d) SNR reflected signal with the adjusted wave.

https://doi.org/10.5194/hess-2019-560
Preprint. Discussion started: 18 November 2019

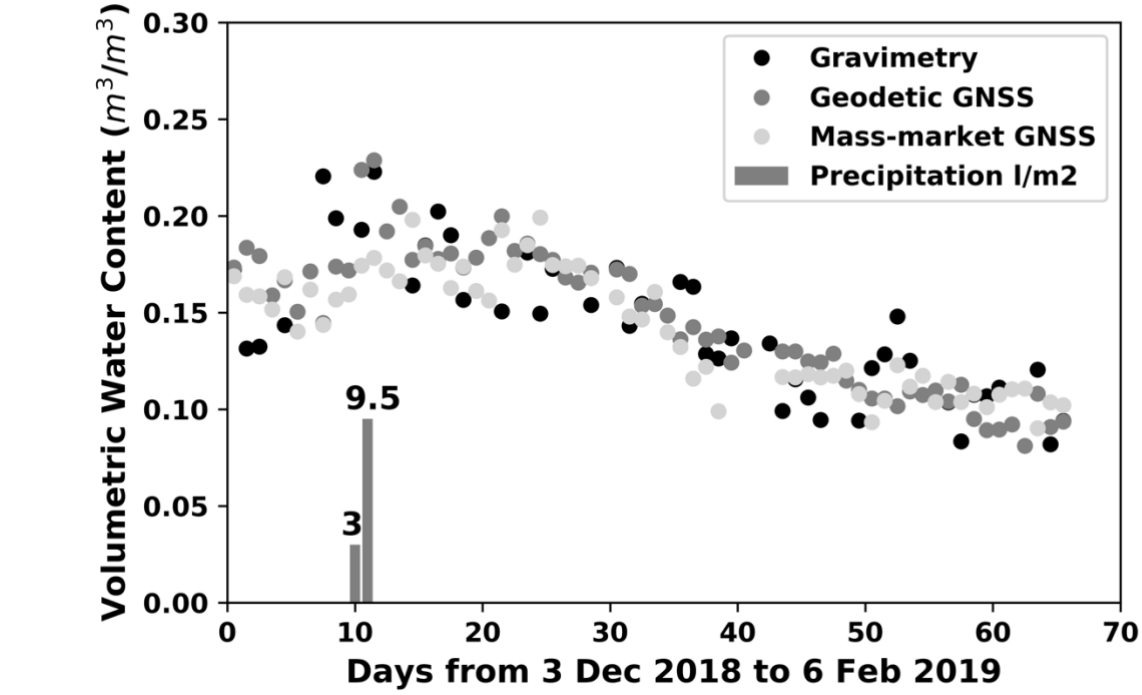

Figure 11. GPS comparison of daily soil moisture. The results of the geodetic and mass-market antennas are compared with the reference gravimetric data set.

https://doi.org/10.5194/hess-2019-560
Preprint. Discussion started: 18 November 2019

Hydrology and Earth System Sciences
Discussions

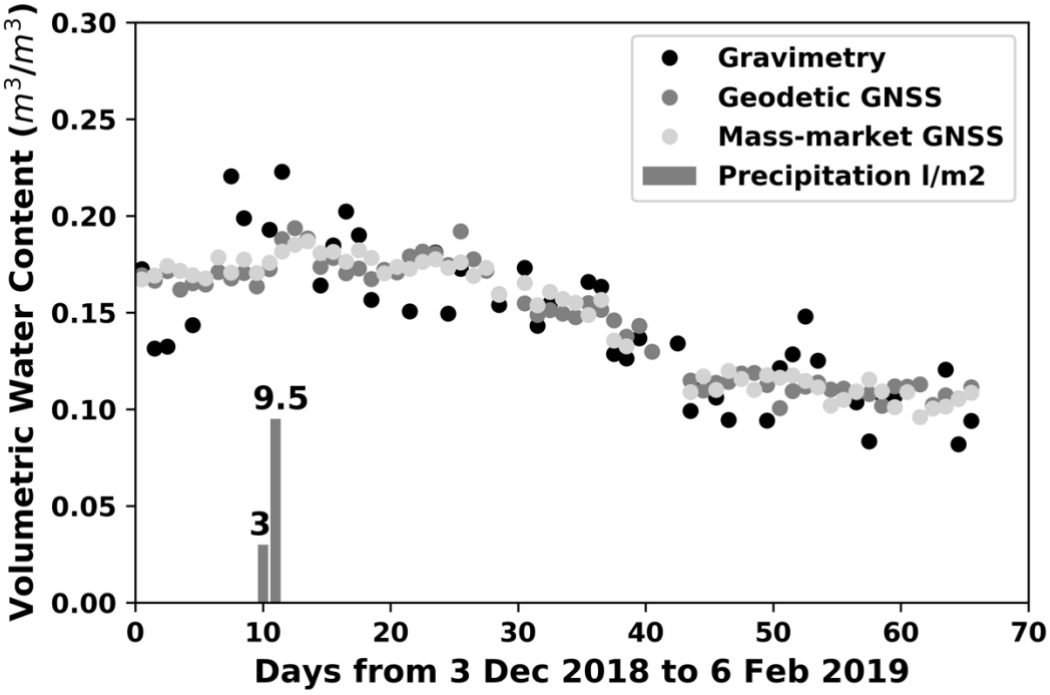

Figure 12. GLONASS comparison of daily soil moisture. The results of the geodetic and mass-market antennas are compared with the reference gravimetric data set.

https://doi.org/10.5194/hess-2019-560
Preprint. Discussion started: 18 November 2019

Hydrology and Earth System Sciences
Discussions
Open Access
EGU

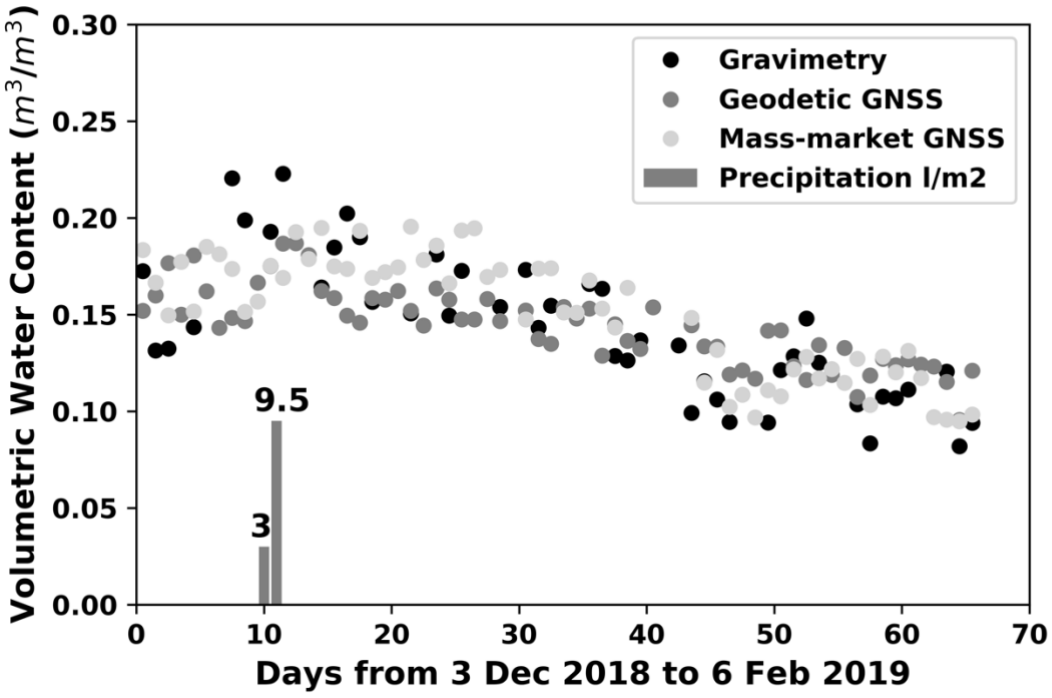

Figure 13. GALILEO comparison of daily soil moisture. The results of the geodetic and mass-market antennas are compared with the reference gravimetric data set.